This article was downloaded by: [Tomsk State University of Control Systems and Radio]
On: 23 February 2013, At: 07:44
Publisher: Taylor & Francis
Informa Ltd Registered in England and Wales Registered Number: 1072954
Registered office: Mortimer House, 37-41 Mortimer Street, London W1T 3JH, UK

Molecular Crystals and Liquid Crystals
Publication details, including instructions for authors and subscription information:
http://www.tandfonline.com/loi/gmcl16

Light Scattering Characteristics in Liquid Crystal Storage Materials

D. Meyerhofer [a] & E. F. Pasierb [a]
[a] RCA Laboratories, Princeton, New Jersey, 08540
Version of record first published: 28 Mar 2007.

To cite this article: D. Meyerhofer & E. F. Pasierb (1973): Light Scattering Characteristics in Liquid Crystal Storage Materials, Molecular Crystals and Liquid Crystals, 20:3-4, 279-300

To link to this article: http://dx.doi.org/10.1080/15421407308083049

PLEASE SCROLL DOWN FOR ARTICLE

Full terms and conditions of use: http://www.tandfonline.com/page/terms-and-conditions

This article may be used for research, teaching, and private study purposes. Any substantial or systematic reproduction, redistribution, reselling, loan, sub-licensing, systematic supply, or distribution in any form to anyone is expressly forbidden.

The publisher does not give any warranty express or implied or make any representation that the contents will be complete or accurate or up to date. The accuracy of any instructions, formulae, and drug doses should be independently verified with primary sources. The publisher shall not be liable for any loss, actions, claims, proceedings, demand, or costs or damages

whatsoever or howsoever caused arising directly or indirectly in connection with or arising out of the use of this material.

Downloaded by [Tomsk State University of Control Systems and Radio] at 07:44 23 February 2013

Molecular Crystals and Liquid Crystals. 1973. Vol. 20, pp. 279–300
Copyright © 1973 Gordon and Breach Science Publishers
Printed in Great Britain

Downloaded by [Tomsk State University of Control Systems and Radio] at 07:44 23 February 2013

Light Scattering Characteristics in Liquid Crystal Storage Materials†

D. MEYERHOFER and E. F. PASIERB

RCA Laboratories
Princeton, New Jersey 08540

Received March 27, 1972; *and in revised form September* 27, 1972

Abstract—The angular dependence of light scattering was measured in liquid crystal storage cells as a function of material and cell parameters. Both the scattering and clear states were investigated. The storage state scattering was found be be relatively independent of the concentration of cholesteric material in the mixture, the direction of the incident light, and the cell thickness. This suggests that the density of scattering centers is highest near the cell walls. The scattering at practical viewing angles (20 to 50° from the incident light) is to a large part due to Bragg scattering of the cholesteric planes.

1. Introduction

The storage effect[1] is one of a number of electro-optic properties of liquid crystals that can be used for display application. It is observed in cells filled with mixtures of nematic and cholesteric materials of negative dielectric anisotropy. The liquid crystal can assume either of two stable states, clear and scattering, and the transition from one to the other is affected by appropriate electric fields. Information is written in only once and is then available for viewing for an indefinite period.

In any scattering-type display, the light intensity seen by the viewer and the contrast depend not only on the driving forces, but also strongly on the angle at which the display is viewed. We have studied this relationship for different storage materials as a function of the various parameters. The results can be explained qualitatively by a simple model of the molecular arrangement. They allow one to design and optimize the display for the desired application.

† Supported by the Air Force Materials Laboratory, Wright-Patterson Air Force Base, under contract F33615-70C-1590.

Downloaded by [Tomsk State University of Control Systems and Radio] at 07:44 23 February 2013

The storage effect was investigated in cells formed by two glass plates separated 5 to 50 μm. Both plates were covered by transparent electrodes, so that the electric fields were normal to the cell. The liquid crystal mixtures used consisted of 1 to 20% cholesteric component in nematic liquids. These mixtures always exhibit cholesteric properties[2] but have considerably lower viscosity than the pure cholesteric component. This means that the material has a faster electro-optic response and requires lower driving fields.

In the clear or non-scattering state, the material forms the planar cholesteric texture.[3] The helical axis lies uniformly perpendicular to the plane of the electrodes while the molecules lie parallel to that plane. Since the optical axis of this uniaxial material is oriented parallel to the helical axis, light is transmitted uniformly through the cell without scattering or birefringence and the cell appears " clear ". Usually, no preferential direction is established in the plane of the cell and one must assume that the molecular axes are oriented randomly in the plane. The orientation must change smoothly from point to point as these fluctuations cannot be observed under a microscope.

The planar texture is obtained from the scattering state by the application of a high frequency field. This frequency is too high to effect any movement of charge so that the field acts only on the dielectric properties of the liquid, and the molecules tend to orient themselves so that the largest dielectric constant is parallel to the field. Since the dielectric anisotropy of the molecules is negative, they align nearly perpendicular to the field, i.e., in the plane parallel to the electrodes. The field itself does not specify any preferred direction within that plane so that the orientation will depend mainly on the wall forces. The cholesteric forces then produce the helical arrangement. After alignment of the molecules and removal of the high frequency field, there is a slight additional change in texture with a small increase in scattering. This is presumably caused by wall forces but the detailed nature of the change is not clear. We will refer to the zero field planar condition as the quiescent state.

When a low-frequency or dc field is applied to the clear quiescent cell, it becomes highly scattering for voltages above a well-defined threshold despite the fact that the dielectric forces alone tend to keep the molecules aligned in the planar texture. It is identical to the

Downloaded by [Tomsk State University of Control Systems and Radio] at 07:44 23 February 2013

situation in nematic materials of negative dielectric anisortopy. The light scattering in this *Dynamic Scattering Mode* (*DSM*)[4] is caused by turbulent liquid flow accompanying movement of charge in the liquid. The light scattering properties of the storage material are expected to be similar to those of the DSM in nematic materials.

When the field is removed and the liquid motion ceases, it reforms a stable cholesteric phase—the scattering or storage state. Because of the " memory " of the turbulent condition, the helical axis is not uniformly oriented but points in different directions in different regions of the cell. This appears to be the well-known *focal conic texture.*[3] The liquid is at rest but scattering of light takes place because of rapid variations of the direction of the " crystalline axis ".

2. Materials

The storage materials studied were selected from a large number of compounds synthesized and evaluated by Castellano and co-workers.[5] The nematic host NH-1 was a mixture of three Schiff-base compounds of the type

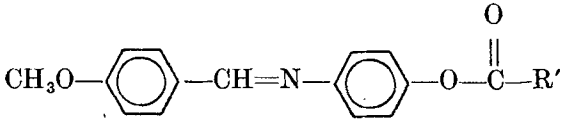

which had the lowest melting point and widest nematic range. It consisted of equivalent quantities of the compounds with R′ being CH_3, C_3H_7, and C_4H_9. The cholesteric compound used was cholesteryl oleate which exhibited the best properties for the storage behavior.[5]

A useful storage effect is observed over the concentration range from 2 to 25% cholesteryl oleate in NH-1. With increasing concentration of the cholesteric component the response of the cells becomes slower, and the storage time longer[5] as might be expected from the increasing viscosity. At the same time the helical pitch of the cholesteric structure, which is inversely related to the optical rotatory power, decreases from infinity at the pure nematic compound towards the value of the cholesteric compound.[6] We have measured the optical repeat distance ($p/2$), which is half the helical pitch,[7] by

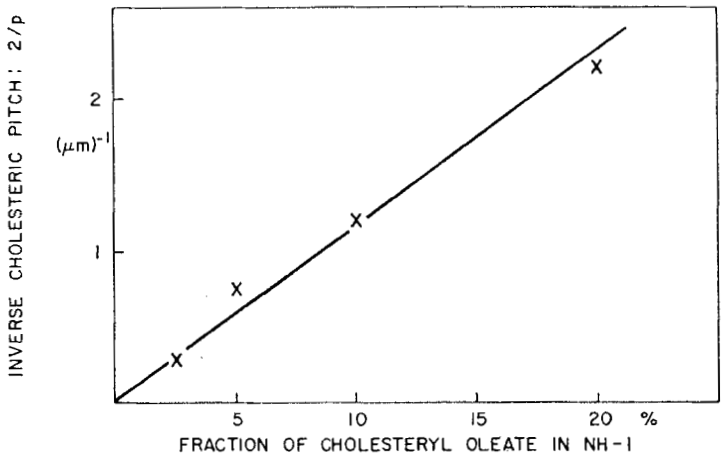

Figure 1. Cholesteric twisting power (reciprocal of the helical pitch p) *versus* concentration of the cholesteric component in the storage mixture.

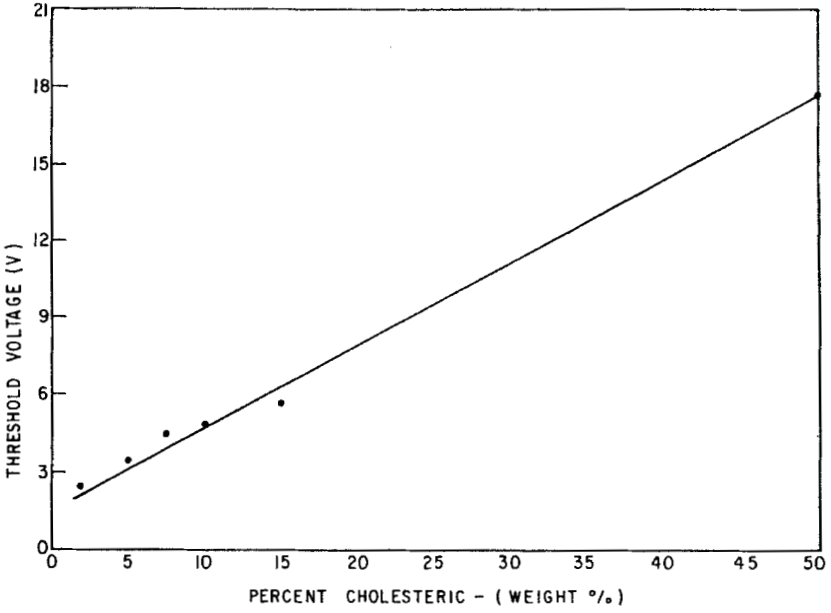

Figure 2. Threshold voltage for dynamic scattering as function of cholesteryl oleate content in NH-1.

Downloaded by [Tomsk State University of Control Systems and Radio] at 07:44 23 February 2013

observing the Grandjean pattern,[8] in a wedged-shaped cell with the planar texture. The molecules are uniformly oriented at the two surfaces by rubbing the glass plates.[6] The wedge angle of the cell is measured by observing the interference pattern produced by HeNe laser light reflected perpendicularly from the two opposing surfaces in a region where there is no liquid. Then the average spacing between two Grandjean lines corresponds to a thickness change of $p/2$.[8] The results are shown in Fig. 1. They approximate the expected linear dependence of $2/p$ on concentration in the range under investigation.[6,9]

The threshold voltage for onset of the DSM state is also concentration dependent as shown in Fig. 2. The threshold for DSM in nematic material is known to depend directly on the viscosity of the material.[10] It is therefore likely that the increase in viscosity with concentration of the mixture is the main reason for the threshold dependence of Fig. 2.

3. Experimental Techniques

The experimental cells consisted of two conducting quartz plates separated by appropriate spacers. The plates are carefully cleaned. No aligning agent is added to the liquid crystal material, and the plates are not rubbed, so that the surface arrangement is random.

The experimental arrangement for measuring the scattering parameters is shown in Fig. 3. The light source is a microscope lamp, collimated so that the light incident on the cell has an angular spread of about 5 deg. Both the angle of incidence (θ) and the angle of measurement (ϕ) could be varied but light propagating outside the plane of the diagram was not considered. For some of the investigations with monochromatic light, a HeNe laser was used and the incident light was then completely collimated.

The scattered light was measured in two different ways. In one method, only part of the cell was illuminated and all the light (scattered into a well-defined solid angle) was measured with a photomultiplier. This produces a value which is easy to interpret physically. In the other technique, the entire cell was illuminated and the brightness measured with a spot brightness meter. This number represents the quantity that a viewer observes in an actual

Downloaded by [Tomsk State University of Control Systems and Radio] at 07:44 23 February 2013

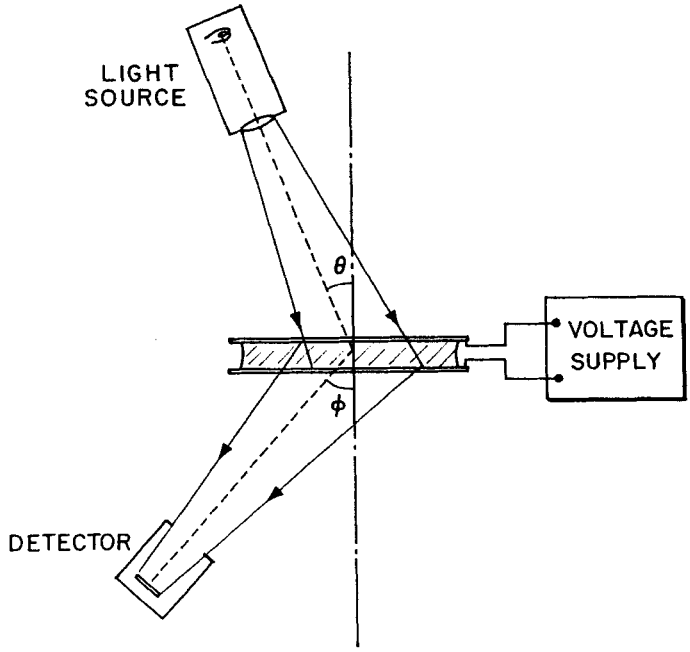

Figure 3. Experimental arrangement for measuring light scattering in liquid crystal cells. Only light propagating in the plane of the diagram is considered.

display. It is related to the first quantity in the following way. The incident light intensity is proportional to $\cos\theta$ because the area illuminated by a fixed section of the beam varies as $1/\cos\theta$. The brightness meter measures the light impinging on it from a fixed solid angle. As the distance to the cell is kept constant, the cell area subtended by the solid angle must vary as $1/\cos\phi$. Consequently, the reading of the brightness meter will be $\cos\theta/\cos\phi$ times the values of the photomultiplier reading.

In making the measurements, care was taken to obtain reproducible results. This meant not only attention to the preparation of the cells, but also applying the various voltages in the same magnitude and in the same time sequence. In this manner, the values in the DSM and in the storage state could be reproduced reliably, particularly those of the scattered light. There tends to be somewhat more fluctuation in the attenuated direct beam.

Downloaded by [Tomsk State University of Control Systems and Radio] at 07:44 23 February 2013

Downloaded by [Tomsk State University of Control Systems and Radio] at 07:44 23 February 2013

4. Angular Dependence of Light Scattering

Typical curves of light scattering as function of viewing angle are shown in Fig. 4 for one cell in three different conditions. In both scattering conditions, one notes a substantial peak near zero angle which represents the attenuated, but unscattered, incoming beam.

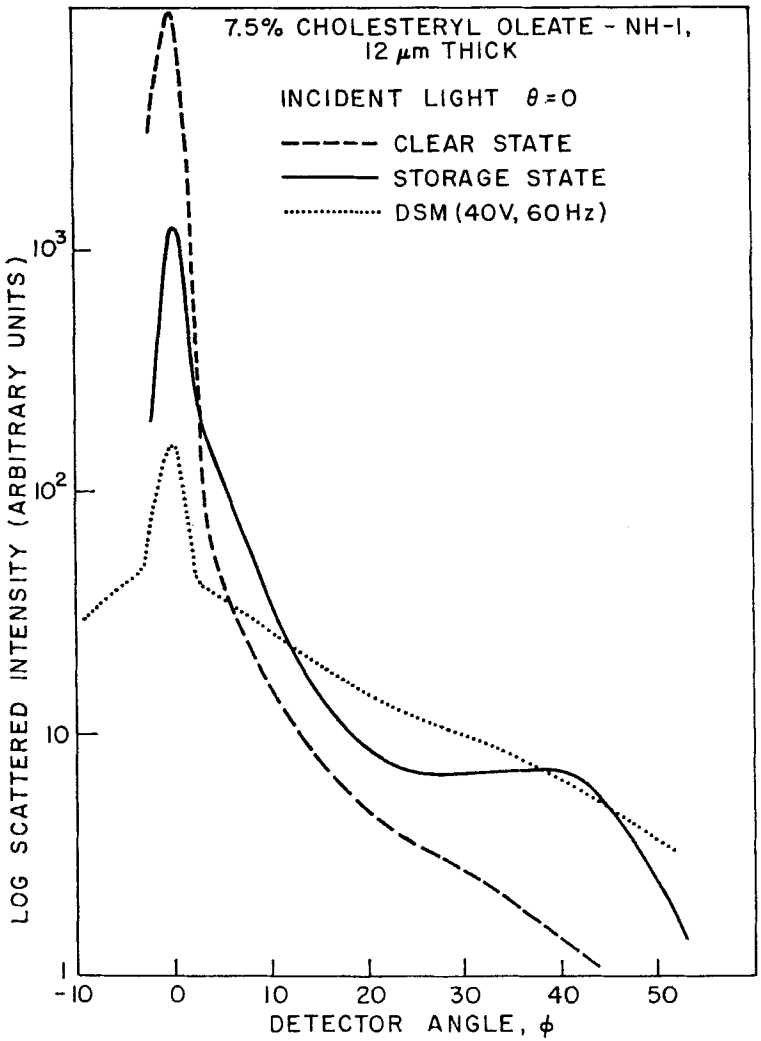

Figure 4. Scattering intensity measured with a photomultiplier vs. detector angle in three different states of operation.

The height of that peak depends strongly on the collimation of the incident beam and disappears when a broad source is used. In any case, the cells appear completely scattering to a visual observer.

The quiescent state still shows some scattering which is the reason for the relatively low contrast ratios of these cells. The degree of this scattering is quite variable from cell to cell. It may be related to the exact treatment of the wall surfaces, although we have not been able to demonstrate this conclusively. The scattering is reduced considerably during the erase cycle with the high frequency field, when the planar texture appears almost transparent. When the field is removed, however, some misalignment takes place with the molecules rotating out of the plane of the cell. The reason for this is not understood at present.

When a low-frequency electric field is applied, an electro-hydrodynamic instability sets in at a well defined threshold voltage. At higher voltages, the liquid flow becomes turbulent and causes dynamic scattering. In the DSM (Fig. 4), the scattering decreases slowly and monotonically with angle. The characteristic is the same as that observed in the DSM of nematic materials with negative dielectric anisotropy. The dependence on voltage, angle, and sample thickness is also similar for the two cases. As an example, the voltage dependence of the DSM in a storage material is shown in Fig. 5.

When the voltage is removed and the turbulent motion ceases, the scattering focal-conic texture is produced. The amount of scattering in the stored state depends only weakly on the magnitude of the previously applied voltage. Figure 4 demonstrates that there are two contributions to the transmitted light: one part which decreases monotonically with scattering angle, and a narrow band located between about 25 and 55°. The narrow band becomes much more pronounced in monochromatic collimated illumination. If, for example, a HeNe laser beam (633 nm) is incident normally on a storage cell of 10% cholesteric component a sharp cone of scattered light is observed forming an angle of 45° with the incident direction. This will be shown to be due to Bragg diffraction by the helical cholesteric structure. The effect is only observed over the range of 5 to 20% of the cholesteric component in the mixture.

For device applications, the most pertinent quantity is the contrast

Downloaded by [Tomsk State University of Control Systems and Radio] at 07:44 23 February 2013

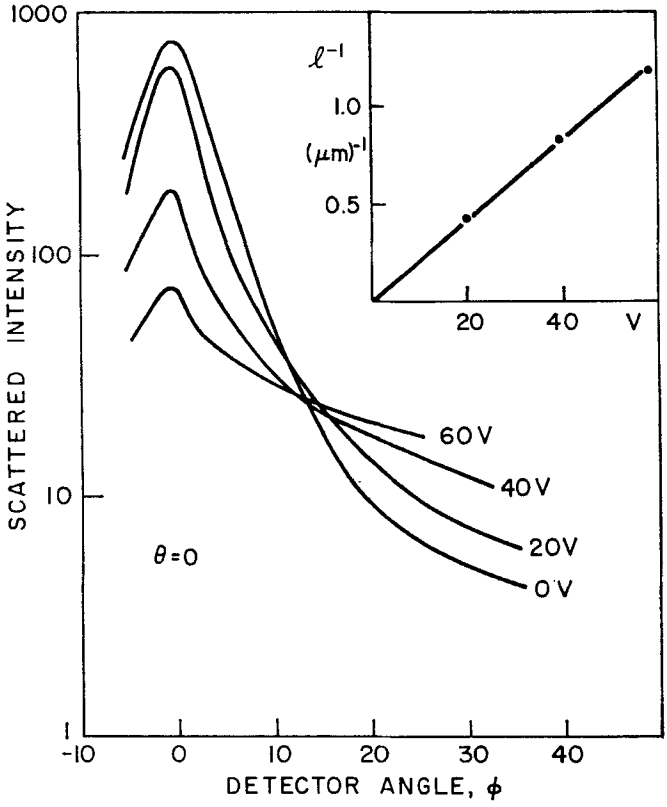

Figure 5. Voltage dependence (60 Hz) of the scattered light intensity in the DSM for a 25 μm thick cell of 10% cholesteryl oleate solution. The insert shows the correlation lengths derived from the scattering curves by Eq. (2).

ratio, namely the ratio of the scattered light in the storage state to that in the quiescent state. This quantity is shown for a 5% cell in Fig. 6. The two curves represent the cases where $\theta = 0°$ and where $\phi = 0°$. (Because these quantities are ratios, the cos θ/cos ϕ term need not be taken into account.) Both curves demonstrate the prominent peak near the Bragg scattering angle. As discussed previously, the contrast ratio is strongly dependent on the perfection of the clear state and, therefore, varies from cell to cell. However, the shape of the curves is typical.

It should be noted, at this point, that both the DSM and the clear planar texture sometimes appear to have a small amount of Bragg

Downloaded by [Tomsk State University of Control Systems and Radio] at 07:44 23 February 2013

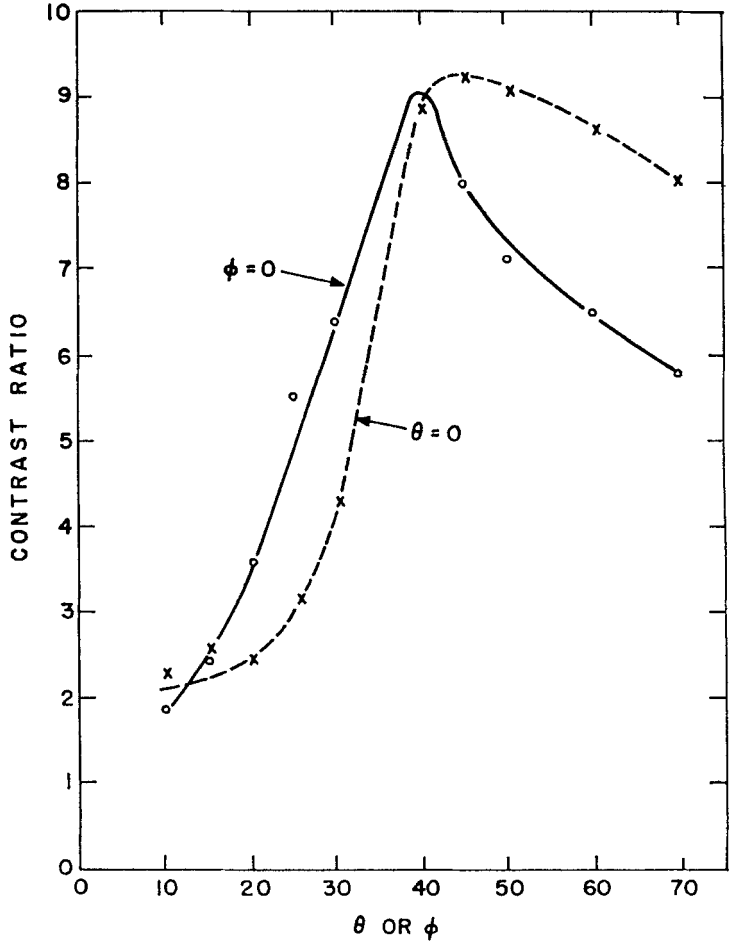

Figure 6. Contrast ratio as function of scattering angle in a 12 μm thick cell of 10% cholesteryl oleate solution. For the solid curve, the detector is located normal to the cell and the angle of illumination (θ) is varied; for the dashed curve, the illumination is normal and the detector is moved.

scattering. For the planar texture, this means that the misorientation mentioned must include some tilt in the helical axis as well as possible distortions at the walls and out of planes parallel to the walls. The flow in the DSM must be sufficiently fast and turbulent so that the helical ordering of the cholesteric phase is almost completely disrupted.

The measurements described up to now were all taken with the

Downloaded by [Tomsk State University of Control Systems and Radio] at 07:44 23 February 2013

illuminating light beam perpendicular to the cells. This is not necessarily the geometrical arrangement in which these cells would be used for storage or display. We, therefore, preformed scattering measurements where both the incoming direction and scattering direction were varied. The storage state scattering curves for two different directions of θ are compared in Fig. 7. They show that the light scattering appears to depend mainly on $(\theta + \phi)$, i.e., on the relative scattering angle from input to output, rather than on the orientation of the cell (θ or ϕ separately). This conclusion is also supported by the two similar curves of Fig. 6.

The dependence on incident angle is investigated in more detail in Fig. 8 where we plot the scattering intensity in the storage state at

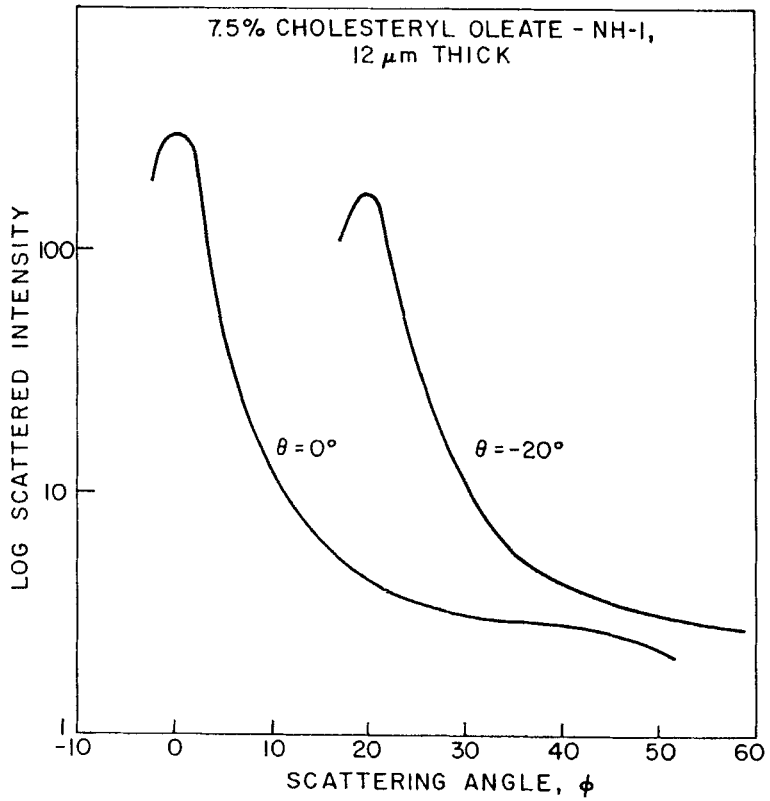

Figure 7. Scattered light distribution in the storage state for two different directions of incident light.

Downloaded by [Tomsk State University of Control Systems and Radio] at 07:44 23 February 2013

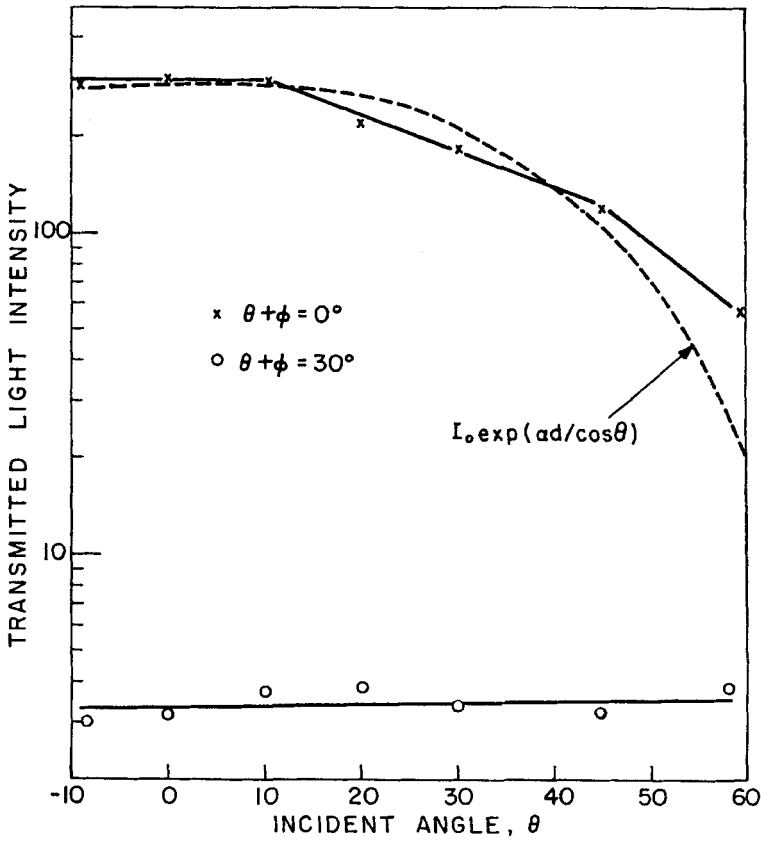

Figure 8. Transmitted light intensity (×) and scattered light intensity at an angle 30° away from the incident angle (○) as a function of the incident angle in the storage state (12 μm thick cell of 7.5% mixture). The dashed curve represents Eq. (2).

two fixed values of $(\theta + \phi)$. First, consider the attenuated direct beam $(\theta + \phi = 0°)$. If the material is uniformly scattering, one expects the attenuation to depend exponentially on thickness. The attenuation coefficient is then

$$\alpha = \frac{\cos\theta}{d} \ln \frac{I_0}{I} \tag{1}$$

This quantity is shown by the dashed curve in Fig. 8, with d adjusted to fit I/I_0 at $\theta = 0°$ (c.f. Table 1). There is qualitative agreement with the experimental points. The situation is quite different for the

Downloaded by [Tomsk State University of Control Systems and Radio] at 07:44 23 February 2013

scattered light. At $\theta + \phi = 30°$, there is no change in the scattered intensity with θ (or with ϕ) even at large angles of incidence. This is also true for other values of $(\theta + \phi) \neq 0$.

TABLE 1 Attenuation of Direct Beam in Storage Cells of Various Thicknesses in the Storage State

	A	B	C
Cell Thickness	$25\,\mu m$	$12\,\mu m$	$6\,\mu m$
Attenuation Ratio	0.038	0.085	0.15
Logarithm (dB)	14.2	10.8	8.1
α	$0.13\,\mu m^{-1}$	$0.21\,\mu m^{-1}$	$0.31\,\mu m^{-1}$

A number of tests were made to compare materials of different compositions. Some results for the storage state are shown in Fig. 9. The curves are very similar in magnitude. However, only the two intermediate concentrations show the Bragg scattering peak, as was mentioned above.

Another practical parameter is the cell thickness. The scattering intensity in the storage state is shown in Fig. 10 for three cells of different thickness. The intensity and angular dependence of the scattered light varies only slightly among the three samples, a rather surprising result. Because the angle of Bragg scattering depends only on the material, one can expect the general shape of the scattering curves to be the same. However, if the scattering centers are uniformly distributed throughout the cells, and of equal density in the different cells, the attenuation of the direct beam must follow Eq. (1). Table 1 lists the average ratio of transmitted to incident beam ($\theta = \phi = 0°$) obtained from Fig. 10 and other data and the corresponding values of α obtained from Eq. (1). Since the latter values vary with thickness, one can not assume that the density of scattering centers is uniform.

One thickness dependent factor does not appear on the curves. For the thinnest ($6\,\mu m$) cells the storage state is not as stable as for the thicker cells. The amount of attenuation of the direct beam varies with time after the cell is activated into the storage mode. There is a partial reversion to the clear state which reaches saturation after about 30 min. This indicates that in these thin cells, the wall forces dominate over the volume forces.

Downloaded by [Tomsk State University of Control Systems and Radio] at 07:44 23 February 2013

Downloaded by [Tomsk State University of Control Systems and Radio] at 07:44 23 February 2013

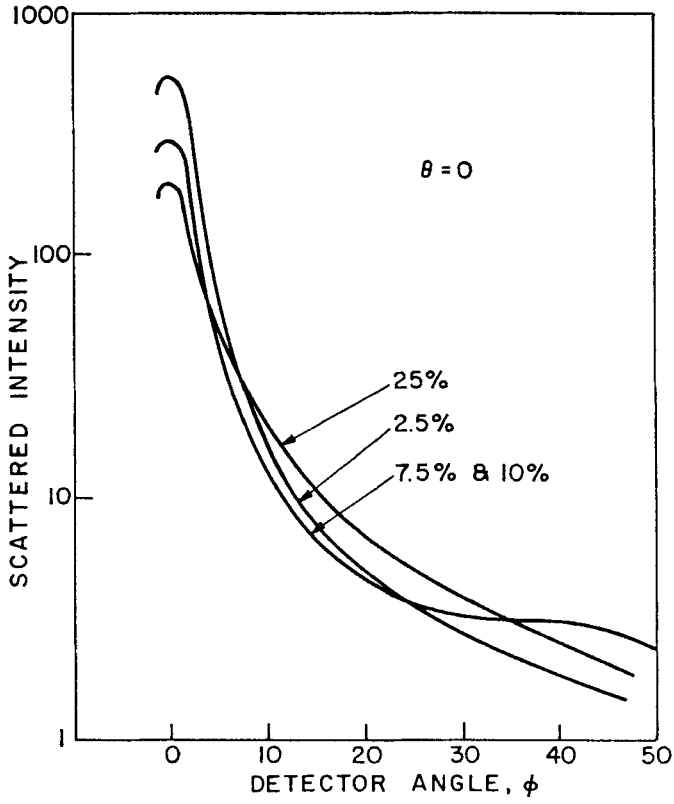

Figure 9. The angular dependence of light scattering for four different concentrations of cholesteryl oleate in NH-1 in the storage state in 12 μm thick cells. The values for the 7.5% and 10% mixtures are the same within experimental accuracy.

Downloaded by [Tomsk State University of Control Systems and Radio] at 07:44 23 February 2013

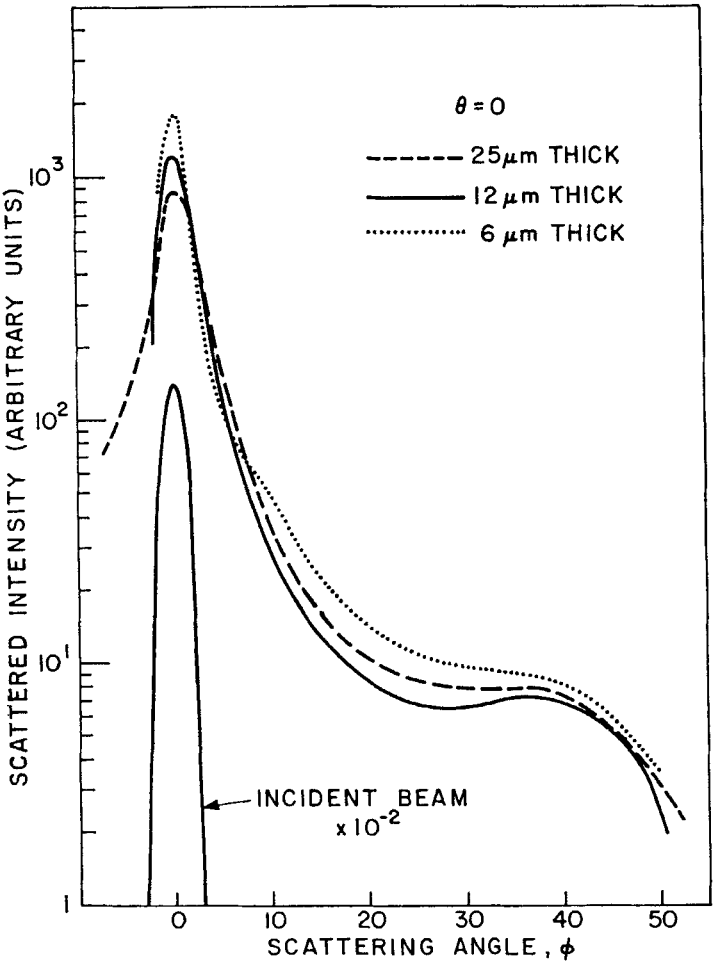

Figure 10. The scattering characteristics of the storage state in cells of different thickness (7.5% cholesteryl oleate in NH-1). Also shown is the intensity of the incident beam attenuated 100 × .

Downloaded by [Tomsk State University of Control Systems and Radio] at 07:44 23 February 2013

5. Interpretation of the Measurements

Consider first what we have called the *dynamic scattering state*, which is produced by a low-frequency field above a certain voltage threshold (Fig. 2). The reason for this assumption is that the scattering behavior in this state is indistinguishable from that observed in the DSM of typical nematic materials, such as MBBA.[11,12] To demonstrate this we will discuss various characteristics of the scattering behavior that the two groups of materials have in common:

(1) After the attenuated direct beam is subtracted from the scattering curve the scattered intensity depends approximately exponentially on angle, the slope decreasing with increasing voltage. Deutsch and Keating[11] express this relationship in the form

$$I/I_0 \approx \exp\left(\frac{l}{\lambda}\phi\right) \tag{2}$$

where l is a coherence length for scattering and is inversely related to the amount of turbulence. The values of l derived from the curves of Fig. 5 are plotted as function of applied voltage in the insert of that figure. A reciprocal relationship is obtained, which is what one might expect from the simplest model in which the fluid velocity is proportional to the applied voltage. It shows that the turbulent regions are of the same order of magnitude as the pitch. This suggests that the cholesteric structure is completely disrupted in the DSM.

(2) For a given material the light scattering as function of angle depends only on the applied voltage.[12] It is independent of the resistivity and the cell thickness. The former implies that the flow of the charge carriers relative to the fluid is unimportant compared to the flow of the fluid itself. This was justified for electrohydrodynamic motion in general by Felici.[13] The thickness independence of the scattering applies not only to the scattered light, but also to the attenuated direct beam (in contrast to the storage state results shown in Table 1). It may be caused by at least two possible effects. First, the fact that the electric field, at a given voltage, is higher in thin cells, produces higher fluid velocity, and increased turbulence. More scattering is caused per unit volume compensating for the reduction of volume with thickness. The difficulty with this ex-

planation is that increased turbulence means a smaller value of l and, from Eq. (2), a smaller slope of the angle-dependence of the scattering for the thinner cells. The measured results show the slope, at a given voltage, to vary little for cells from 6 to 25 μm thick. A different explanation is based on a model where the flow is relatively uniform and smooth in the interior of the cells, and most of the turbulence and scattering takes place in layers near the surfaces. These layers could be approximately the same for all thicknesses. The difficulty here is to derive the dependence of turbulence on voltage or field.

(3) The amount of scattering depends only on the scattering angle *relative* to the incident direction,[12] and not on the orientation of the cell relative to the incident light in agreement with the storage state results. This confirms that the thin film approximation[11] may be applied to the scattering.[14] It supports the second explanation in (2) which assigns most of the scattering to thin layers in the cell.

Consider next what happens when the driving field is turned off. The liquid stops moving and the structure which was previously disturbed by shear forces relaxes to a less-disturbed cholesteric arrangement. Because the cholesteric axis will point in different directions in various parts of the fluid we expect the *focal-conic texture* to be formed. The size of the individual " domains " may be related to the size of the vortices in the turbulent state; but the observation that the scattering does not depend strongly on the voltage applied previously in the DSM, suggests that the focal-conic texture takes on some equilibrium structure, determined by material and, possibly, cell thickness.

The " domain " picture is confirmed by the cone of scattered light observed in the storage state, in the intermediate concentration range. It is closely related to Bragg scattering in powder X-ray pictures. The model for it is shown in Fig. 11. While in the focal-conic texture the direction of the helical axis varies continuously through the material, we have assumed that it may be approximated by a " polycrystalline " material with small randomly oriented " crystallites ". These are one-dimensional, rather than three-dimensional " crystallites " since the periodicity exists only along the helical axis. The scattering planes, in which the molecular axes point along a fixed line, are indicated in the figure. They lie perpendicular to the helical axis and are separated by $p/2$.[7] The

Downloaded by [Tomsk State University of Control Systems and Radio] at 07:44 23 February 2013

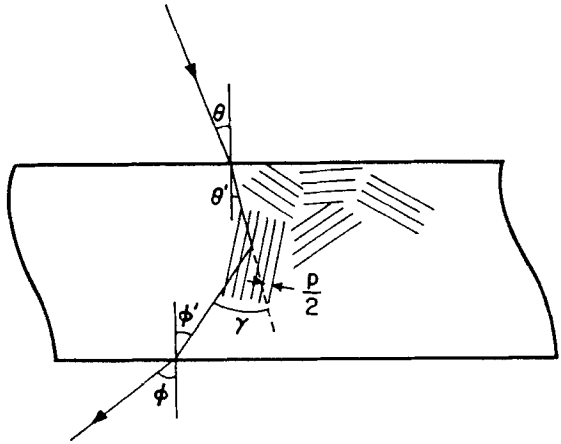

Figure 11. Schematic drawing of Bragg scattering in the focal-conic texture.

diffraction cones appear because there are always some " crystallites " oriented so as to fulfill the Bragg scattering equation

$$\lambda' = \left(\frac{p}{2}\right) 2 \sin \frac{\gamma}{2} \tag{3}$$

as shown in Fig. 11. Here, λ' is the wavelength in the medium ($\lambda' \approx \lambda/n$, where n is the average refractive index) and θ' and ϕ' are the interior angles, related to θ and ϕ by Snell's law. $\gamma = \theta' + \phi'$. For normal incidence ($\theta = 0$) and

$$\lambda' = p \sin \frac{\phi'}{2} \tag{4}$$

or, approximately, the scattering angle is

$$\phi = 2\lambda/p \tag{5}$$

For a 10% mixture $p/2 = 0.83\,\mu$m (Fig. 1), so that for light of $0.633\,\mu$m wavelength, $\phi = 48°$, which compares with the cone angle of 45° measured with the HeNe laser. For white light peaking at $0.55\,\mu$m the angle will be somewhat smaller in adequate agreement with the various bands on the scattering curves.

There is another way in which the scattering in the Fig. 11 model differs from the powder X-ray scattering. In the latter, the condition $\lambda \sim a \ll s$ applies, where a is the dimension of the periodicity, or the unit cell, and s is the size of the crystallite. In the focal-conic

Downloaded by [Tomsk State University of Control Systems and Radio] at 07:44 23 February 2013

texture we have only $\lambda \sim p \sim s$, at least for thin cells, where s can be no larger than the thickness. This causes a spreading of the diffracted beam from the well-defined cone, for two reasons:

(1) In a thin cell we can approximate the model of Fig. 11 by a two-dimensional structure, where the " crystallites " occupy the entire thickness. Then it is obvious, that each cell, of lateral dimension s, acts as an aperture, in addition to its scattering properties. Because $\lambda \sim s$ this causes diffraction spreading of both the direct beam and the scattered beams. The spread is given by

$$\Delta\phi_{\text{diffr.}} \approx \lambda/s \tag{6}$$

(2) In Bragg scattering Eq. (3) applies precisely only for an infinitely large grating. Here individual " crystallites " contain only a few planes, since $s \sim p$. The diffraction in such a system was calculated by Kogelnik[15] who showed that the spread about the Bragg angle is given by

$$\Delta\phi_{\text{Bragg}} \approx -p/2s \tag{7}$$

in the simplest case.

In our mixtures we have $p/2 > \lambda$ so that it is $\Delta\phi_{\text{Bragg}}$ which makes the large contribution. From the experimental curves (e.g., Fig. 6) we can estimate for mixtures of 5 to 20% cholesteric, which show the Bragg scattering, that $\Delta\phi_{\text{Bragg}} \approx 0.5$. This implies from Eq. (7) that the average cell dimension, s, is about $2\,\mu$m, which agrees quite well with typical dimensions of the turbulent vortices.

We can now see why the Bragg-scattered light is only observed in a certain concentration range. For mixtures with less than 5% cholesteric component in the DSM $p/2$ becomes larger than s and $\Delta\phi > \phi$ so that the cone of scattering is completely smeared out and can no longer be observed. In contrast to this, at concentrations of more than 20% cholesteric, $p/2$ becomes smaller than λ', and ϕ' approaches the angle of total internal reflection. The Bragg-scattered light is no longer transmitted.

It is also possible to see why we do not observe any chromatic effects, despite the fact that optical diffraction plays an important part in the scattering. We calculate the difference in scattering angle at different wavelengths approximately from Eq. (5) as

$$\Delta\phi_\lambda = \phi(\lambda_1) - \phi(\lambda_2) = 2\Delta\lambda/p \tag{8}$$

Downloaded by [Tomsk State University of Control Systems and Radio] at 07:44 23 February 2013

For white light of $\Delta\lambda = 0.2\,\mu$m and $p/2 = 1\,\mu$m, $\Delta\phi_\lambda = 0.2$, which is considerably smaller than the spreading due to the diffraction effects. This means that the chromatic spreading is completely smeared out.

From the attenuation results (Table 1) it appears that the structure of the texture varies with cell thickness and this may be expressed in a variation of s. Unfortunately one cannot derive sufficiently accurate values of $\Delta\phi$ from the experimental curves to determine the dependence of s on cell thickness.

Consider finally the *quiescent state*. Here the grating planes are all parallel to the cell walls, and any Bragg scattering appears on the same side as the incident light. Because of the refraction at the air-cell interface the minimum diffraction angle γ which can be observed externally (at smaller angles the rays are totally reflected at the interface) is

$$\gamma/2 \geqslant \cos^{-1}(1/n) \tag{9}$$

Using Eq. (3) we find that light of wavelength λ will only be observed externally, if

$$\frac{p}{2} \leqslant \frac{\lambda}{2\sqrt{n^2-1}} \tag{10}$$

Thus, no visible light is seen unless $p/2 \gtrsim 0.3\,\mu$m. This does not happen in the concentration range investigated here, in agreement with the observations.

6. Discussion

A number of features emerge from the scattering measurements which have application to the design of cells for optimum display characteristics. Most importantly, the scattering of the storage state does not depend much on either the proportion of cholesteric material in the mixture or on the cell thickness. Since both of these variables have important influences on other properties of the cells, particularly the response speed, one will be able to select the parameter values to optimize these other properties.

The contrast ratio, for a given material, is mainly determined by the scattering of the quiescent state. What controls this variable

Downloaded by [Tomsk State University of Control Systems and Radio] at 07:44 23 February 2013

property is not clear, but it appears to be related to surface effects. Further investigation of methods to treat the surface is required.

One of the major material parameters that influences the scattering of the storage state is the pitch of the cholesteric helix. We have seen that the Bragg scattering produces a large fraction of the light intensity at typical viewing angles. Values up to 40 or 50° will generally be required for viewing by transmitted light so that the value of the helical pitch p should be about $1.5\,\mu$m.

Acknowledgements

This investigation was suggested by J. A. Castellano and benefited from numerous discussions with him and with A. Sussman.

Downloaded by [Tomsk State University of Control Systems and Radio] at 07:44 23 February 2013

REFERENCES

1. Heilmeier, G. H. and Goldmacher, J. E., *Proc. IEEE* **57**, 34 (1969).
2. Friedel, G., *Ann. Physique* **18**, 273 (1922).
3. Haas, W., Adams, J. A. and Flannery, J. B., *Phys. Rev. Lett.* **24**, 577 (1970).
4. Heilmeier, G. H., Barton, L. A. and Zanoni, L. A., *Proc. IEEE* **56**, 1162 (1968).
5. Castellano, J. A. *et al.*, to be published.
6. Cano, R. and Chatelain, P., *Comp. Rend.* **253**, 1815 (1961).
7. The optical repeat distance of the cholesteric structure is half the pitch p of the helix since two planes perpendicular to the helical axis, which are separated by a distance $p/2$, contain molecules oriented along the same direction. The symmetry of the structure is such that one cannot distinguish between the two opposite orientations of the molecular axes.
8. Grandjean, F., *Comp. Rend.* **172**, 71 (1921).
9. Nakagiri, T., *Phys. Lett.* **36A**, 427 (1971).
10. Helfrich, W., *J. Chem. Phys.* **51**, 4092 (1969).
11. Deutsch, Ch. and Keating, P. N., *J. Appl. Phys.* **40**, 4049 (1969).
12. Meyerhofer, D., unpublished data.
13. Felici, N., *Rev. Gen. Elec.* **78**, 717 (1969).
14. This can be seen most simply if the scattering liquid is modeled by an assembly of spheres with diameter of the order of the coherence length l. The spheres replace the vortices of the turbulent, birefringent liquid. Then a lightbeam incident on a thick layer will be scattered many times (each scattering event having the appropriate statistical distribution of angle changes) and when it leaves the cell its direction will no longer depend on the direction at which it was incident (θ). Consequently the statistical distribution of exiting light will also be independent of θ and

only depend on ϕ. In contrast the thin film case allows only one scattering event and it is the change of angle that is statistically determined for the one event. The exiting light will therefore depend on the relative angle change $\theta + \phi$, which is what is observed experimentally.

15. Kogelnik, H., *Bell Syst. Tech. J.* **48**, 2909 (1969).

Downloaded by [Tomsk State University of Control Systems and Radio] at 07:44 23 February 2013